

# Crystal Structure and Vibrational Spectra of Poly(trimethylene terephthalate) from Periodic Density Functional Theory Calculations

Daria Galimberti and Alberto Milani\*

Dipartimento di Chimica, Materiali, Ingegneria Chimica “Giulio Natta”, Politecnico di Milano, Piazza Leonardo da Vinci 32, 20133 Milan, Italy

## I. INTRODUCTION

Aromatic polyesters are a well-known class of polymeric materials whose application is now widespread in our everyday life, as witnessed by poly(ethylene terephthalate) (PET) and its countless applications. These polymers show peculiar properties such as even–odd effects depending on the number of methylene units between aromatic rings, resulting in a different conformation and different mechanical behavior for individual members of this family, and even some subtle polymorphic transitions. Indeed, the second member of this family in order of technological importance, poly(butylene terephthalate) (PBT), shows a reversible transition between different crystal structures upon mechanical deformation due to a variation in the conformation of the chain.<sup>1–6</sup> On the other hand, poly(trimethylene terephthalate), PTT, the aromatic polyester containing three methylene units between the aromatic rings, has received much less attention with respect to PET and PBT. This is mainly due to the fact that it has become available at low cost only recently, paving the way to its technological application for commercial production. The physicochemical and mechanical properties of PTT are different from those of PET and PBT and show promising potentialities for its applications.

As for other classes of polymers, vibrational spectroscopy techniques have been usually adopted to investigate the properties of these polyesters. However, these investigations have been based exclusively on experimental works or

semiempirical calculations, and it is thus quite common to find different interpretations and also some ambiguities in the past literature.

In this context, computational techniques which can give a reliable description of both the structural and vibrational properties of the system became available only very recently.<sup>7–13</sup>

Therefore, in this work we applied these state-of-the-art techniques to carry out periodic density functional theory (DFT) calculations augmented with an empirical dispersion correction (DFT-D)<sup>14,15</sup> of poly(trimethylene terephthalate) by using the CRYSTAL09 code,<sup>16,17</sup> to investigate both the structural and vibrational properties of PTT. Actually, the CRYSTAL code has been successfully applied to a few polymer systems, namely, to the case of polystyrene,<sup>7–9</sup> polyglycine,<sup>10</sup> nylon 6 polymorphs,<sup>11</sup> nylon 6,6,<sup>12</sup> and poly(tetrafluoroethylene),<sup>13</sup> where it allowed solution of open questions in the interpretation of the structural and vibrational properties, offering computational tools not available before.

Our aims are 2-fold: from one hand, since PTT has been much less studied than PET or PBT, we investigate its structural and vibrational properties to unveil some uncertainties in the interpretation of its IR spectra and to give a

**Received:** November 25, 2013

**Revised:** January 16, 2014

**Table 1. Summary of the Numerical Values Adopted in Calculations (Cases 1–3; See Text) for the Parameters Occurring in Grimme’s Correction for Dispersion Interactions<sup>a</sup>**

	$D$	$s_6$	$C_6^H$	$C_6^C$	$C_6^O$	$C_6^N$	$R_{vdW}^H$	$R_{vdW}^C$	$R_{vdW}^O$	$R_{vdW}^N$
case 1	20	1.05	0.14	1.75	0.70	1.23	1.001	1.452	1.342	1.397
case 2	20	1.00	0.14	1.75	0.70	1.23	1.3013	1.5246	1.4091	1.4668
case 3	20	1.00	0.14	1.75	0.70	1.23	1.3013	1.70	1.52	1.55

<sup>a</sup>In all cases, a cutoff distance of 25.0 Å was used to truncate direct lattice summation.  $C_6$  are in units of J nm<sup>6</sup> mol<sup>-1</sup> while  $R_{vdW}$  are in unit of Å.

contribution for better insight into its properties. On the other hand, due to the absence of polymorphism effects, PTT is the ideal test case to set up the computational parameters before extending the same methodology to much more complicated systems, such as PBT and its polymorphic transitions, which will be the subject of future investigations.

To these aims, in section III.1 the DFT-D computed crystal structure of PTT will be compared with the available experimental data, discussing also the importance of different computational parameters, such as the basis set choice or the parameters adopted in Grimme’s correction for dispersion interactions.<sup>14,15,18</sup> On the basis of this structural investigation, in section III.2 the IR spectra of the PTT crystal will be predicted and compared with previous experimental studies taken from the literature.<sup>19–26</sup>

## II. COMPUTATIONAL DETAILS

Full geometry optimization of the crystal structure and the calculation of the IR spectra of PTT have been carried out by means of the CRYSTAL09 code<sup>16,17</sup> in the framework of DFT. We adopted the B3LYP<sup>27,28</sup> hybrid exchange-correlation functional together with the 6-31G(d,p) basis set and the recently developed pob-TZVP<sup>29</sup> basis set that has been explicitly parametrized for CRYSTAL periodic calculations. In all calculations the B3LYP functional has been used augmented with an empirical correction for dispersion interaction (B3LYP-D) proposed by Grimme<sup>14,15</sup> and implemented in CRYSTAL09. Due to the possibility of a choice of different sets of empirical parameters in the model, three different cases have been considered and compared in the present investigation as also done in previous works.<sup>11–13</sup> The numerical values of these parameters are reported in Table 1: (case 1) parameters proposed by Grimme in his original work;<sup>14,15</sup> (case 2) parameters proposed by Civalleri et al.;<sup>18</sup> (case 3) same parameters as those in case 2 except van der Waals (vdW) radii of C, N, and O which have been fixed to the standard values reported by Bondi.<sup>30,31</sup>

In all calculations, the atomic positions and the lattice parameters were fully optimized; default optimization algorithms and convergence criteria were adopted.

In the case of PTT, only one stable form has been found and no other polymorph has been observed: two independent resolved structures have been proposed in the literature by Poulin-Dandurand et al.<sup>32</sup> and Desborough et al.,<sup>33</sup> and both agree in predicting a triclinic unit cell with  $P\bar{1}$  space group and TGGT conformation on the methylene chain. In our case, as starting guess structure for the calculations, we considered the experimentally determined crystal parameters and atomic coordinates reported by Poulin-Dandurand et al.<sup>32</sup> As already proposed in previous works<sup>11–13</sup> and as explained in section III.2, in order to detect the spectroscopic markers of regularity/crystallinity, we carried out also geometry optimization and frequency calculation on the infinite polymer chain characterized by a regular conformation (one-dimensional (1D)

model chain), taking as the starting structure the conformation shown by the chain in the crystal. The optimized PTT crystal structure is sketched in Figure 1.

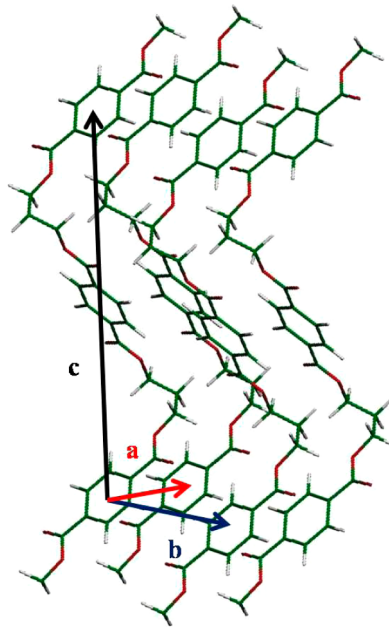


**Figure 1.** Sketch of the crystalline structure of PTT.

Normal frequency calculations at the  $\Gamma$  point have been carried out on the optimized geometries as achieved by diagonalization of the (numerically calculated) Hessian matrix.

The DFT-D computed spectra have been compared with experimental IR spectra taken from the literature.<sup>19–26</sup> In these previous works, the authors focused respectively on different frequency ranges when analyzing the vibrational properties of PTT; therefore, when our results are compared with the experimental ones, IR spectra recorded by different authors have been plotted in the different figures depending on the spectral region under investigation.

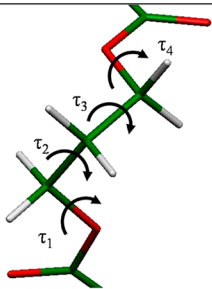
From now on, for the sake of simplicity, we will indicate as B3LYP-D(cX) the DFT calculation carried out by including Grimme’s correction using “case X” ( $X = 1, 2, 3$ ) parameters reported in Table 1. To compare the computed and the experimental data, the calculated frequencies B3LYP-D(c3)/6-31G(d,p) (which is the method adopted for the interpretation of the vibrational properties of PTT; see the next section) were scaled by 0.9713. This scaling factor has been determined to put the DFT computed C=O stretching band in correspondence of the experimental reference bands found at 1710 cm<sup>-1</sup> by many authors,<sup>19,20,22</sup> and it has been used both for the crystal and the 1D chain model.

**Table 2. Experimental<sup>32,33</sup> and B3LYP-D Computed Cell Parameters for PTT<sup>a</sup>**

	expt		6-31G(d,p)			pob-TZVP		
	ref 32	ref 33	c1	c2	c3	c1	c2	c3
<i>a</i>	4.637	4.600	4.162	4.331	4.386	4.367	4.461	4.514
<i>b</i>	6.266	6.200	5.983	6.482	6.540	6.089	6.229	6.267
<i>c</i>	18.640	18.300	18.322	18.056	18.377	16.909	17.011	17.191
$\alpha$	98.400	98.000	96.513	100.982	101.004	98.037	98.906	99.079
$\beta$	93.000	90.000	90.609	89.903	89.973	90.172	90.094	90.078
$\gamma$	111.100	112.000	112.061	116.218	116.462	112.459	112.218	112.127
Percent Errors								
<i>a</i>			-10.253	-6.595	-5.410	-5.830	-3.806	-2.652
<i>b</i>			-4.518	3.448	4.371	-2.830	-0.592	0.015
<i>c</i>			-1.706	-3.133	-1.410	-9.287	-8.737	-7.773
$\alpha$			-1.918	2.624	2.647	-0.369	0.514	0.690
$\beta$			-2.571	-3.330	-3.255	-3.041	-3.125	-3.142
$\gamma$			0.865	4.607	4.827	1.223	1.006	0.925
Average Percent Errors								
			3.639	3.956	3.653	3.763	2.963	2.533

<sup>a</sup>Distances are in Å; angles, in degrees. Percent errors and the average percent errors with respect to the structure reported in ref 32 are reported for each case.

**Table 3. Experimental<sup>32,33</sup> and B3LYP-D(c3) Computed Dihedral Angles for the Alkyl Sequence of the PTT Chain<sup>a</sup>**

	Exp. <sup>32</sup>	Exp. <sup>33</sup>	6-31G(d,p)	pob-TZVP	
$\tau_1$	168	167	164	174	
$\tau_2$	60	73	58	62	
$\tau_3$	60	61	67	63	
$\tau_4$	170	152	172	176	

<sup>a</sup>Angles in degrees.

### III. RESULTS AND DISCUSSION

**III.1. Crystalline Structure.** In Table 2 we report the values of the cell parameters obtained by full geometry optimization by using different parameters for Grimme's correction and two basis sets (6-31G(d,p) and pob-TZVP). These values are compared to the experimental ones reported by Poulin-Dandurand et al.;<sup>32</sup> the percent errors for each case have also been estimated.

In previous papers on Nylon 6<sup>11</sup> and Nylon 6,6,<sup>12</sup> a very good agreement has been found with experimental values when the B3LYP/6-31G(d,p) level of theory is employed, and the best results have been reached by using case 3 parameters for Grimme's correction [B3LYP-D(c3)/6-31G(d,p)]. This trend is confirmed for PTT, even if now also B3LYP-D(c1) is a good approximation in addition to B3LYP-D(c3), with an average error over all the cell parameters of 3.639.

Furthermore, our DFT calculations confirm that the PTT chains in the crystal possess a TGGT conformation on the alkyl part as reported in Table 3.

However, it should be noted that B3LYP-D(c1) shows much larger errors if only *a* and *b* parameters are considered: in these cases, the DFT results largely underestimated the experimental values. This trend has been found also in other cases when the parameters proposed by Grimme in his original work (that is B3LYP-D(c1))<sup>11,12,18</sup> are used; in fact these parameters are

known to overcorrect the dispersion interaction, and *a* and *b* cell parameters are indeed related to the intermolecular weak packing of the chains and are significantly influenced by Grimme's correction.

On this basis, we find again that B3LYP-D(c3) parameters can be considered the best choice of the three. In this work we also repeated the calculations by employing the recently developed pob-TZVP basis set,<sup>29</sup> explicitly parametrized to be used in periodic calculations with CRYSTAL09 code. Due to the fact that this basis set is more extended than 6-31G(d,p) and it has been adapted for CRYSTAL calculations, we should expect better agreement with the experimental results.

Actually, when considering B3LYP-D(c2) and B3LYP-D(c3), the average error is further reduced and now B3LYP-D(c3)/pob-TZVP is the best choice among all of the ones here investigated. In particular, the percent errors on *a* and *b* parameters are now almost half with respect to the 6-31G(d,p) case; this result is quite straightforward since a larger basis set such as pob-TZVP largely reduces effects such as basis set superposition error which are more effective on those parameters that are related to intermolecular packing. However, an unexpected result is found in the case of the *c* parameter, associated with the chain axis: when using the pob-TZVP basis set, the percent errors now drastically increase in all cases and are around 7–9%, much larger than the 1.5–3% error found for

the 6-31G(d,p) basis set. The reasons for such discrepancies are unknown, and other systems should be analyzed to verify if some systematic errors are present for this basis set, maybe due to the fact that it has been developed and tested only for ionic solids, semiconductors, and metals.<sup>29</sup> Since  $c$  parameter is directly related to the chain axis and thus to the intramolecular interactions, the ones which mainly affect the vibrational properties of this system, we preferred to adopt the B3LYP-D(c3)/6-31G(d,p) level of theory for analysis of the IR spectra of PTT rather than the B3LYP-D(c3)/pob-TZVP level. Very good predictions of the IR spectra have been indeed obtained for other polymers already at the 6-31G(d,p) level;<sup>7–13</sup> the next analysis of IR spectra of PTT will be thus based on B3LYP-D(c3)/6-31G(d,p) data.

**III.2. Prediction of the IR Spectra.** On the basis of the structural optimization discussed in the previous section, we here analyze in detail the vibrational features of PTT and in particular its IR spectra: in the literature, even if in the case of PTT no polymorphism effect is observed, some discrepancies are present in the spectroscopic assignments. As mentioned above, the DFT spectra reported here are those obtained at the B3LYP-D(c3)/6-31G(d,p) level of theory. In any case, despite the large error on the  $c$  parameter, similar results are obtained also when the pob-TZVP basis set is used (see the Supporting Information).

In Figures 2–5, the DFT computed spectra for the PTT crystals are compared in different frequency ranges with the

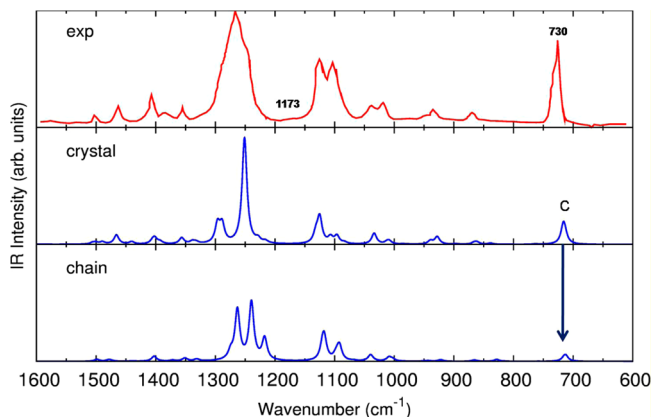


**Figure 2.** Comparison of the experimental spectrum of Bulkin et al.<sup>19</sup> and the B3LYP-D(c3)/6-31G(d,p) spectra computed for the crystal and the 1D chain model in the frequency range of 600–1600 cm<sup>-1</sup>.

experimental IR spectra reported in the literature by different authors;<sup>19,20,25</sup> in addition to the spectrum computed for the crystal, also the spectrum of the regular infinite chain model is shown to discuss the importance of intermolecular interaction on the vibrational properties of crystalline PPT.

Since the birth of polymers' vibrational spectroscopy, the theoretical treatment of the vibrational problem of crystalline polymers has been carried out by choosing a single, infinite chain model possessing the same conformation observed in the crystal (see for example refs 34 and 35 for a general discussion). The rationale behind this choice is related to the fact that the vibrational properties are mostly influenced by intramolecular interactions, while intermolecular interactions can be considered as a small perturbation. Obviously, this approximation can be very crude in some cases (for example hydrogen-bonded polymers) where intermolecular effects can heavily affect the

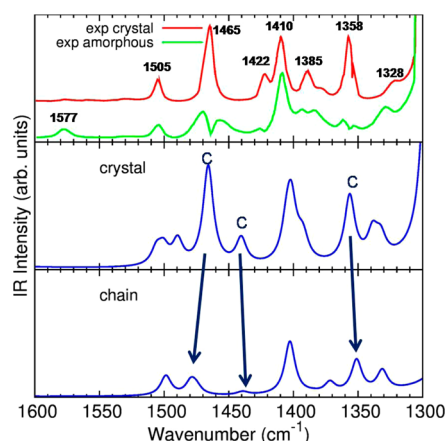


**Figure 3.** Comparison of the experimental spectra of Kim et al.<sup>20</sup> and the B3LYP-D(c3)/6-31G(d,p) spectra computed for the crystal and the 1D chain model in the frequency range of 1300–1600 cm<sup>-1</sup>.

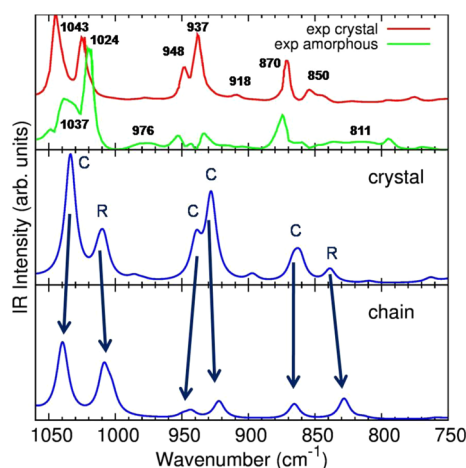


**Figure 4.** Comparison of the experimental spectra of Kim et al.<sup>20</sup> and the B3LYP-D(c3)/6-31G(d,p) spectra computed for the crystal and the 1D chain model in the frequency range of 750–1050 cm<sup>-1</sup>.

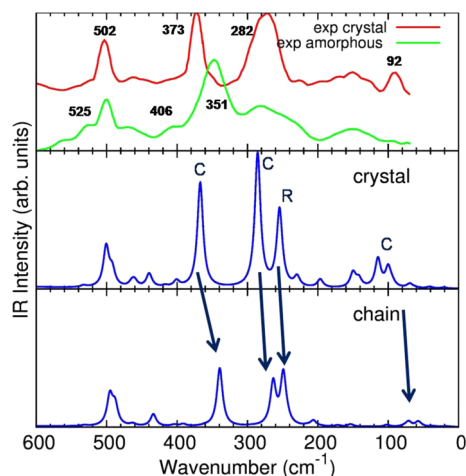


**Figure 5.** Comparison of the experimental spectra of Vasanthan et al.<sup>25</sup> and the B3LYP-D(c3)/6-31G(d,p) spectra computed for the crystal and the 1D chain model in the frequency range of 0–600 cm<sup>-1</sup>.

vibrational spectra. Furthermore, even some features (e.g., crystal-field splitting) observed in the IR spectrum of the simplest polymer, polyethylene, are due to supramolecular

effects (i.e., the presence of more than one molecule in the unit cell). As a further aspect, in this ground a debate took place in past literature about the so-called “regularity” and “crystallinity” bands: indeed, when considering the vibrational spectra of crystalline polymers, it is important to distinguish between those bands which are effectively due to the presence of a long-range tridimensional order (i.e., crystallinity bands) and those bands which are due only to the fact that the chains possess a regular conformation (i.e., regularity), independently of their supramolecular packing in a crystal lattice. The latter ones cannot be necessarily markers also of the presence of 3D crystals since they are the result only of the intramolecular order. In other words, regularity bands are already present in smectic phases simply characterized by orientational order and by the presence of “elongated” chains with regular conformation (e.g., quenched polypropylene) as well as for stretch oriented polymers where the occurrence of elongated conformations (e.g., transplanar polymethylenes chains or helix conformations) versus coiled chains should be distinguished from recrystallization in 3D lamellar domains. Therefore, these differences have a practical outcome: when using bands for a quantitative estimate of the crystallinity degree, it should be taken into consideration the fact that a regularity band cannot be a true marker of the crystalline phase since it is independent of the molecular packing of the chains and it is only sensitive to the regular intramolecular structure. In order to assign the bands as regularity vs crystallinity bands, the spectrum of the crystal should be compared to the spectrum of the 1D model chain: those bands whose pattern in frequency and/or intensity and/or band shape is markedly different in the two cases are indeed crystallinity bands since they are largely affected by the crystal packing (e.g., the intensification of IR absorptions have been found for hydrogen-bonded polymers such as nylons,<sup>11,12</sup> and crystal-field band splitting is observed in polyethylene); on the other hand, those bands which have a similar pattern in the two spectra should be considered as regularity bands, since they are only affected by the existence of a peculiar regular conformation of the chains, independently of their intermolecular environment. Also in the case of PTT, we will see that the interactions between the chains in the crystal will influence significantly the IR spectrum, allowing a clear discrimination between crystallinity and regularity bands.

In all of the figures here displayed, very good agreement between experimental and DFT computed spectra is found: the spectrum computed for the crystal actually reproduces the experimental results also in the minor features and provides a detailed interpretation and assignment of the marker bands without taking into account standard empirical correlations which could give place to uncertainties and ambiguities.

In Figure 2 we compare the DFT spectra with the experimental spectrum reported by Bulkin et al.<sup>19</sup> in the frequency range of 600–1800  $\text{cm}^{-1}$ : the good agreement between DFT and experimental spectra can be immediately verified. From this general comparison we can already confirm one of the previous assignments: it has been proposed by different authors<sup>19–22,26</sup> that an experimental band occurring at 1173  $\text{cm}^{-1}$  should be assigned to trans conformation in the amorphous phase. In our calculations, no bands are predicting in this range, thus supporting the previous assignment to the amorphous phase. Furthermore, we can also corroborate the suggestion that the band at 730  $\text{cm}^{-1}$  receives contributions both from the amorphous and the crystalline phases as stated

by Ward and Wilding,<sup>23</sup> thought it should be remarked that the main contribution comes from the amorphous one.

In order to proceed further in a detailed assignment, in Figures 3 and 4 we analyze separately the 1300–1600 and 600–1050  $\text{cm}^{-1}$  frequency ranges, comparing the DFT spectrum of the crystal with the experimental spectra reported by Kim et al.<sup>20</sup> who analyzed these regions in detail. The region between 1300 and 1200  $\text{cm}^{-1}$  will be not commented on in detail since a very strong and broad band is present in the experimental spectra; this band is due to both crystalline and amorphous domains, and it is thus not significant, neither for the quantitative determination of the amount of the amorphous/crystalline phase in different samples nor to investigate the intra- or intermolecular properties of PTT in different phases.

In the range of 1300–1600  $\text{cm}^{-1}$ , the band at 1577  $\text{cm}^{-1}$  has been found to decrease with annealing and has been assigned by Kim to the amorphous phase. A similar result has been reported also by other authors:<sup>22,26</sup> also in this case no bands are predicted, thus supporting this previous assignment.

Considering now the band observed at 1465  $\text{cm}^{-1}$ , we can verify that this band is a significant marker of the crystalline phase (computed band at 1466  $\text{cm}^{-1}$ ). In the experimental spectra, this band actually consistently increases upon annealing while in the amorphous spectra only a broad band with two main components at 1469 and 1458  $\text{cm}^{-1}$  is observed.<sup>19,20,22,26</sup> The comparison between the crystal and the 1D chain model reveals that this band gathers intensity in the crystal and it is thus a true crystallinity band. The intensification that is found for many crystallinity bands of PTT can be related to the existence of quite significant interactions among the chains in the crystals. This is also proved by the red shift predicted for the C=O stretching band at 1710  $\text{cm}^{-1}$  of the crystal with respect to the 1D model chain (1750  $\text{cm}^{-1}$ ): this shift points out the existence of nonnegligible local intermolecular interactions which are responsible for the modulation of the IR spectrum of the crystal. Another band, which usually is assigned as a marker of the crystalline phase, is the strong one observed at 1358  $\text{cm}^{-1}$ ; many authors<sup>19–24,26</sup> assign this feature to a wagging mode of the  $\text{CH}_2$  in a TGGT gauche conformation, while Lee et al.<sup>24</sup> assigned it as a marker of a GTTG trans conformation. Our calculations indicate that this band (computed at 1356  $\text{cm}^{-1}$ ) is an evident marker of the PTT crystalline phase and confirm its assignment to the TGGT conformation, which is the one observed in the crystal also in our calculations (the sketch of the normal mode is reported in the Supporting Information). This classification is particularly significant also for practical and analytical purposes since this band has been proposed as a marker to evaluate quantitatively the amount of gauche conformers present in a sample.<sup>22</sup> It must be noted that, even if this band is quite strong also in the single chain spectrum, it is intensified by the crystalline field and thus it is a crystallinity band. Another band which has a significant intensity both in the experiments and calculations is the band observed at 1410  $\text{cm}^{-1}$ . This feature, associated with aromatic ring vibrations, is predicted by the convolution of two bands calculated at 1405 and 1403  $\text{cm}^{-1}$ . This band, however, is present for both amorphous and crystalline phases and should be thus treated as a reference band. Considering then the band experimentally observed by some authors at 1385  $\text{cm}^{-1}$ , this band has been usually associated with the amorphous phase<sup>20–22,24</sup> and in particular with GTTG trans conformers<sup>22</sup> or TGGT gauche conformations.<sup>24</sup> Kim et al.<sup>20</sup> showed that in

**Table 4. Classification of Marker Bands of PTT Crystal<sup>a</sup>**

exptl freq (cm <sup>-1</sup> )	previous classification	B3LYP-D(c3)/6-31G(d,p) freq (scaled by 0.9713; cm <sup>-1</sup> )	B3LYP-D(c3)/6-31G(d,p) IR intensity (km/mol)	new classification
92	crystal <sup>25</sup>	convolution		crystal (crystallinity)
		100	12	
		115	18	
282	crystal <sup>25</sup>	254{249}	48{32}	crystal (crystallinity/regularity)
		285	83	
351	amorphous <sup>25</sup>			amorphous
373	crystal <sup>25</sup>	367	66	crystal (crystallinity)
525	amorphous <sup>25</sup>			amorphous
811	amorphous <sup>21,22,26</sup>			amorphous
850	crystal <sup>20,23</sup>	839{828}	23{36}	crystal (regularity)
870	crystal + amorphous <sup>20</sup>	convolution		crystal (crystallinity)
		861	41	
		866	33	
937	crystal <sup>19-22,26</sup>	928	149	crystal (crystallinity)
948	crystal <sup>19-22,26</sup>	939	68	crystal (crystallinity)
976	amorphous <sup>20,22,26</sup>			amorphous
1024	crystal <sup>20,22</sup>	convolution		crystal (regularity)
		1009{1003}	59{35}	
		1012{1009}	35{78}	
1173	amorphous <sup>19-22,26</sup>			amorphous
1037/1043	crystal <sup>20-23,26</sup>	1034	218	crystal (crystallinity)
1328	amorphous <sup>20,22,26</sup>	convolution		significant contributions due to crystal
		1332	38	
		1339	49	
1358	crystal <sup>19-24,26</sup>	1356	122	crystal (crystallinity)
1385/1389	amorphous <sup>19-22,26</sup> /crystal <sup>20</sup>	shoulder		amorphous with small crystal contribution
		1392	38	
1410	reference band <sup>19,24</sup>	convolution		reference band
		1403	107	
		1405	56	
1422	crystal <sup>20</sup>	1440	48	crystal (crystallinity)
1465	crystal <sup>19,20,22,26</sup>	1466	184	crystal (crystallinity)
1505	crystal, <sup>21</sup> ref <sup>20,22</sup>	1506	29	contributions due to crystal
1577	amorphous <sup>20,22,26</sup>			amorphous
1710	reference band <sup>19,22</sup>	convolution		reference band
		1710	1048	
		1711	1024	

<sup>a</sup>The computed frequencies [B3LYP-D(c3)/6-31G(d,p)] refer to the calculation on the crystal. In the case of “regularity” bands the computed value according to the model of the isolated chain (1D model) is also reported in {} brackets. In the Supporting Information the sketch of the normal mode associated with each band is reported.

the same range a band at 1389 cm<sup>-1</sup> is observed for the crystal and another one at 1393 cm<sup>-1</sup> is observed for the amorphous. The DFT spectrum shows (at 1392 cm<sup>-1</sup>) a shoulder of the main features at 1405 cm<sup>-1</sup> which could indicate indeed that in this region a contribution of the crystalline phase is present. However, due to the simultaneous presence of bands of the two phases, this spectral range is not significant for quantitative measurements. In this frequency range three other bands should be taken into account, observed respectively at 1328, 1422, and 1505 cm<sup>-1</sup>. The first one is found to decrease with annealing, and therefore it has been assigned to the amorphous phase;<sup>20,22,26</sup> our calculation reveals that the two bands at 1332 and 1339 cm<sup>-1</sup> can be put in correspondence with this frequency value, thus indicating that the experimental band at 1328 cm<sup>-1</sup> cannot be assigned uniquely to the amorphous phase.

In the case of the weak band at 1422 cm<sup>-1</sup>, our calculation corroborates the assignment to the crystalline phase proposed by Kim et al.:<sup>20</sup> a band is predicted at 1440 cm<sup>-1</sup> which can be

put in correspondence with this band; moreover by comparison with the 1D chain model, we can state that it is a true crystallinity band. Finally, the band at 1505 cm<sup>-1</sup> has been assigned to the crystal phase by Chuah<sup>21</sup> and as a reference band by other authors:<sup>20,22</sup> our calculation reveals that the crystal gives contribution to this band (1506 cm<sup>-1</sup>).

Another frequency range where significant markers of the crystal and amorphous phase are found is the 600–1050 cm<sup>-1</sup> region (Figure 4). Here again very good agreement between experimental and DFT spectra is found. Going into detail, the band at about 1043 cm<sup>-1</sup> is assigned to the crystalline phase by many authors (with small differences in frequency (1043<sup>20,22,23</sup> and 1037 cm<sup>-1</sup><sup>19,21,26</sup>) while a shoulder at slightly lower frequency is reported for the amorphous phase.<sup>20-23,26</sup> DFT calculations confirm its assignment to the crystal phase (band calculated at 1034 cm<sup>-1</sup>). Comparison with the 1D chain model reveals that this band is enhanced in intensity in the crystal, and it is thus a crystallinity band. A second band is predicted at about 1010 cm<sup>-1</sup> (convolution of the two bands computed at



1012 and 1009  $\text{cm}^{-1}$ ) which can be put in correspondence with the experimental bands at 1024  $\text{cm}^{-1}$ . Some authors<sup>20,22</sup> assigned this band to the crystalline phase; however, at 1018  $\text{cm}^{-1}$  another band is observed for the amorphous phase,<sup>19,20,22</sup> and thus we do not believe that this feature could be used for quantitative measurements of the crystallinity percentage due to this bands overlap. In any case, the band predicted at 1010  $\text{cm}^{-1}$  is a regularity band, since its intensity does not show an increase with respect to the corresponding band of the 1D model chain (convolution of two bands predicted at 1003 and 1009  $\text{cm}^{-1}$ ). The doublet observed at about 940  $\text{cm}^{-1}$  is also very well predicted by the calculations. The two experimental bands at 948 and 937/933  $\text{cm}^{-1}$  have been assigned in the past as markers of gauche conformations in the crystal phase<sup>19–22,26</sup> although some discrepancies are found among the authors:<sup>23,26</sup> at 933  $\text{cm}^{-1}$  also a contribution due to the amorphous phase is present, and thus the assignment of this band from experimental data is quite ambiguous. DFT calculations indicate that both bands (calculated at 939 and 928  $\text{cm}^{-1}$ ) are indeed markers of the crystalline packing.

In the literature, a very important marker of the amorphous phase/trans conformation, which is also used for quantitative analysis, is the band at 976  $\text{cm}^{-1}$ .<sup>20,22,26</sup> Our predicted spectra show only a very weak band in this region (986  $\text{cm}^{-1}$ ), thus confirming the assignment to the amorphous phase. A similar situation occurs for the experimental band at 811  $\text{cm}^{-1}$ <sup>121–23,26</sup> not predicted by the calculation and thus marker of the amorphous phase. Another doublet is observed at about 860  $\text{cm}^{-1}$  with two components at about 850 and 870  $\text{cm}^{-1}$ . Based on DFT calculations, both bands (computed at 863 and 839  $\text{cm}^{-1}$ ) contribute to the crystal spectrum in agreement with previous assignments,<sup>20,23</sup> even if for the higher frequency components also the contribution of the amorphous takes place.<sup>20</sup> However, only the higher frequency band is a true crystallinity band (convolution of two bands at 866 and 861  $\text{cm}^{-1}$ ) while the one corresponding to the experimental band at 850  $\text{cm}^{-1}$  is indeed a regularity band (839  $\text{cm}^{-1}$ ).

Finally, Yamen et al.<sup>22</sup> assigned a band at 918  $\text{cm}^{-1}$  to the amorphous phase: in our calculations a weak band is calculated at 897  $\text{cm}^{-1}$  which could be put in correspondence with this experimental band, thus indicating that this feature is not only due to the amorphous phase.

The last frequency range here discussed is the far-IR region below 600  $\text{cm}^{-1}$  (Figure 5), which has been experimentally investigated by Vasanthan and Yaman.<sup>25</sup> Starting from the lower frequency, we confirm that the broad 92  $\text{cm}^{-1}$  band, which increases with annealing, is indeed associated with the crystal (115 and 100  $\text{cm}^{-1}$  bands). The same behavior is shown by the 282 and 373  $\text{cm}^{-1}$  bands which are thus a marker of the crystal phase (computed bands at 285 and 254  $\text{cm}^{-1}$  for the experimental 282  $\text{cm}^{-1}$  band and 367  $\text{cm}^{-1}$  for the 373  $\text{cm}^{-1}$  band). In the case of the 92 and 373  $\text{cm}^{-1}$  bands the calculation on the 1D model chain reveals that these are actually crystallinity bands while the 282  $\text{cm}^{-1}$  band is associated with two contributions, a higher frequency crystallinity one and a regularity one. No features are computed that can be put in correspondence with the 351 and 525  $\text{cm}^{-1}$  bands, thus confirming their assignment to the amorphous phase.<sup>25</sup> For the experimental band at 502  $\text{cm}^{-1}$  taking contribution both from the amorphous and crystalline regions we verified that indeed a large contribution of the crystal can be expected (band computed at 501  $\text{cm}^{-1}$ ) while the experimental band at 406

$\text{cm}^{-1}$  is not uniquely due to the amorphous phase since a weak band is predicted at 401  $\text{cm}^{-1}$  for the crystal.

Based on the whole preceding discussion, the final classification of the main IR bands of PTT is reported in Table 4.

## IV. CONCLUSION AND PERSPECTIVES

In this work, we investigated the structural and vibrational properties of a terephthalate polyester, poly(trimethylene terephthalate), PTT, by means of state-of-the-art periodic DFT calculations. As for the other polymer systems investigated by a similar methodology,<sup>7,8,11–13</sup> a detailed interpretation of PTT properties has been obtained, solving the ambiguities and the open questions which are often found in past literature. The attention has been focused here mainly on the vibrational properties of PTT and on the assignment of its IR spectrum: vibrational spectroscopies are indeed extremely sensitive to intra- and intermolecular properties, allowing an investigation of many peculiar phenomena, such as polymorphism and phase transitions. Furthermore vibrational spectroscopy techniques are widely used also in the industrial environment where they are employed both for qualitative and quantitative analyses: the importance of a correct interpretation of the IR spectra is thus well-evident and highlights the significant role played by reliable computational tools. On these grounds, the CRYSTAL code proved to be very powerful in predicting both the crystal structure and the IR spectra of polymer crystals, providing an answer to several open questions.

The present work opens the way to different future possibilities: on one hand, the simple case of PTT demonstrated the reliability of periodic DFT calculations for the investigation of polyesters and they could be extended to the investigation of more subtle phenomena in similar systems, such as for example the polymorphic transitions promoted in poly(butylene terephthalate) by mechanical deformation.<sup>1–6</sup> On the other hand, based on the very good results obtained for PTT and other different polymers, the same methodology can be extended to any other crystalline polymers, both to give an interpretation of the properties of the material and to carry out an investigation of the molecular phenomena involved or to support experimental techniques in the development and characterization of innovative polymeric systems.

## ■ ASSOCIATED CONTENT

### 📄 Supporting Information

Tables listing DFT optimized values of the cell parameters and coordinates of PTT crystal and chain, DFT computed frequencies and IR intensities of PTT crystal and chain, and sketches of the normal modes of vibration of PTT crystal and a figure comparing DFT computed IR spectra by using 6-31G(d,p) and pob-TZVP basis set.

## ■ AUTHOR INFORMATION

### Corresponding Author

\*Tel.: +39-02-23993383. E-mail: alberto.milani@polimi.it.

### Notes

The authors declare no competing financial interest.

## ACKNOWLEDGMENTS

We gratefully thank Prof. Chiara Castiglioni (Politecnico of Milan) for very useful suggestions and discussions during the work and the writing of the paper.

## REFERENCES

- (1) Yokouchi, M.; Sakakibara, Y.; Chatani, Y.; Tadokoro, H.; Tanaka, T.; Yoda, K. Structures of Two Crystalline Forms of Poly(butylene terephthalate) and Reversible Transition between Them by Mechanical Deformation. *Macromolecules* **1976**, *9*, 266–273.
- (2) Dobrovolny-Marand, E.; Hsu, S.; Shih, C. Spectroscopic Characterization of the  $\alpha \rightleftharpoons \beta$  Crystalline Phase Transition in Poly(butylene terephthalate) and Its Copolymers with Poly(tetramethylene oxide). *Macromolecules* **1987**, *20*, 1022–1029.
- (3) Stambaugh, B.; Koenig, J. L.; Lando, J. B. X-ray Investigation of the Structure of Poly(tetramethylene terephthalate). *J. Polym. Sci., Polym. Phys. Ed.* **1979**, *17*, 1053–1062.
- (4) Hall, I. H.; Pass, M. G. Chain Conformation of Poly(tetramethylene terephthalate) and Its Change with Strain. *Polymer* **1976**, *17*, 807–816.
- (5) Desborough, I. J.; Hall, I. H. A Comparison of Published Crystalline Structures of Poly(tetramethylene terephthalate). *Polymer* **1977**, *18*, 825–830.
- (6) Nitzsche, S. A.; Wang, Y. K.; Hsu, S. L. Application of the Molecular Simulation Technique for Clarification of the  $\alpha \leftrightarrow \beta$  Phase Transformation in Poly(butylene terephthalate). *Macromolecules* **1992**, *25*, 2397–2400.
- (7) Torres, F. J.; Civalleri, B.; Meyer, A.; Musto, P.; Albunia, A. R.; Rizzo, P.; Guerra, G. Normal Vibrational Analysis of the Syndiotactic Polystyrene S(2/1)2 Helix. *J. Phys. Chem. B* **2009**, *113*, 5059–5071.
- (8) Torres, F. J.; Civalleri, B.; Pisani, C.; Musto, P.; Albunia, A. R.; Guerra, G. Normal Vibrational Analysis of a Trans-planar Syndiotactic Polystyrene Chain. *J. Phys. Chem. B* **2007**, *111*, 6327–6335.
- (9) Albunia, A. R.; Rizzo, P.; Guerra, G.; Torres, F. J.; Civalleri, B.; Zicovich-Wilson, C. M. Uniplanar Orientations as a Tool to Assign Vibrational Modes of Polymer Chain. *Macromolecules* **2007**, *40*, 3895–3897.
- (10) Ferrari, A. M.; Civalleri, B.; Dovesi, R. Ab Initio Periodic Study of the Conformational Behavior of Glycine Helical Homopeptides. *J. Comput. Chem.* **2010**, *31*, 1777–1784.
- (11) Quarti, C.; Milani, A.; Civalleri, B.; Orlando, R.; Castiglioni, C. Ab Initio Calculation of the Crystalline Structure and IR Spectrum of Polymers: Nylon 6 Polymorphs. *J. Phys. Chem. B* **2012**, *116*, 8299–8311.
- (12) Galimberti, D.; Quarti, C.; Milani, A.; Brambilla, L.; Civalleri, B.; Castiglioni, C. IR Spectroscopy of Crystalline Polymers from ab Initio Calculations: Nylon 6,6. *Vib. Spectrosc.* **2013**, *66*, 83–92.
- (13) Quarti, C.; Milani, A.; Castiglioni, C. Ab Initio Calculation of the IR Spectrum of PTFE: Helical Symmetry and Defects. *J. Phys. Chem. B* **2013**, *117*, 706–718.
- (14) Grimme, S. Accurate Description of van Der Waals Complexes by Density Functional Theory Including Empirical Corrections. *J. Comput. Chem.* **2004**, *25*, 1463–1473.
- (15) Grimme, S. Semiempirical GGA-type Density Functional Constructed with a Long-Range Dispersion Correction. *J. Comput. Chem.* **2006**, *27*, 1787–1799.
- (16) Dovesi, R.; Orlando, R.; Civalleri, B.; Roetti, C.; Saunders, V. R.; Zicovich-Wilson, C. M. CRYSTAL: A Computational Tool for the ab Initio Study of the Electronic Properties of Crystals. *Z. Kristallogr.* **2005**, *220*, 571–573.
- (17) Dovesi, R.; Saunders, V. R.; Roetti, C.; Orlando, R.; Zicovich-Wilson, C. M.; Pascale, F.; Civalleri, B.; Doll, K.; Harrison, N. M.; Bush, I. J.; et al. *CRYSTAL09 User's Manual*; University of Torino: Torino, Italy, 2009.
- (18) Civalleri, B.; Zicovich-Wilson, C. M.; Valenzano, L.; Ugliengo, P. B3LYP Augmented with an Empirical Dispersion Term (B3LYP-D\*) as Applied to Molecular Crystals. *CrystEngComm* **2008**, *10*, 405–410.
- (19) Bulkin, B.; Lewin, M.; Kim, J. Crystallization Kinetics of Poly(propylene terephthalate) Studied by Rapid-Scanning Raman Spectroscopy and FT-IR Spectroscopy. *Macromolecules* **1987**, *20*, 830–835.
- (20) Kim, K. J.; Bae, J. H.; Kim, Y. H. Infrared Spectroscopic Analysis of Poly(trimethylene terephthalate). *Polymer* **2001**, *42*, 1023–1033.
- (21) Chuah, H. H. Orientation and Structure Development in Poly(trimethylene terephthalate) Tensile Drawing. *Macromolecules* **2001**, *34*, 6985–6993.
- (22) Yamen, M.; Ozkaya, S.; Vasanthan, N. Structural and Conformational Changes During Thermally-induced Crystallization of Poly(trimethylene terephthalate) by Infrared Spectroscopy. *J. Polym. Sci., Part B: Polym. Phys.* **2008**, *46*, 1497–1504.
- (23) Ward, I. M.; Wilding, M. A. Infra-red and Raman Spectra of Poly(m-methylene terephthalate) Polymers. *Polymer* **1977**, *18*, 327–335.
- (24) Lee, H. S.; Park, S. C.; Kim, Y. H. Structural Changes of Poly(trimethylene terephthalate) Film Upon Uniaxial and Biaxial Drawing. *Macromolecules* **2000**, *33*, 7994–8001.
- (25) Vasanthan, N.; Yaman, M. Crystallization Studies of Poly(trimethylene terephthalate) Using Thermal Analysis and Far-Infrared Spectroscopy. *J. Polym. Sci., Part B: Polym. Phys.* **2007**, *45*, 1675–1682.
- (26) Vasanthan, N.; Ozkaya, S.; Yaman, M. Morphological and Conformational Changes of Poly(trimethylene terephthalate) during Isothermal Melt Crystallization. *J. Phys. Chem. B* **2010**, *114*, 13069–13075.
- (27) Becke, A. Density-Functional Thermochemistry. 3. The Role of Exact Exchange. *J. Chem. Phys.* **1993**, *98*, 5648–5652.
- (28) Lee, C.; Yang, W.; Parr, R. Development of the Colle-Salvetti Correlation-Energy Formula into a Functional of the Electron-Density. *Phys. Rev. B* **1988**, *37*, 785–789.
- (29) Peintinger, M. F.; Oliveira, D. V.; Bredow, T. Consistent Gaussian Basis Sets of Triple-Zeta Valence with Polarization Quality for Solid-State Calculations. *J. Comput. Chem.* **2013**, *34*, 451–459.
- (30) Bondi, A. Van Der Waals Volumes and Radii. *J. Phys. Chem.* **1964**, *68*, 441–451.
- (31) Rowland, R. S.; Taylor, R. Intermolecular Nonbonded Contact Distances in Organic Crystal Structures: Comparison with Distances Expected from van Der Waals Radii. *J. Phys. Chem.* **1996**, *100*, 7384–7391.
- (32) Poulin-Dandurand, S.; Pérez, S.; Revol, J.-F.; Brisse, F. The Crystal Structure of Poly(trimethylene terephthalate) by X-ray and Electron Diffraction. *Polymer* **1979**, *20*, 419–426.
- (33) Desborough, I. J.; Hall, I. H.; Neisser, J. Z. The Structure of Poly(trimethylene terephthalate). *Polymer* **1979**, *20*, 545–552.
- (34) Painter, P. C.; Coleman, M. M.; Koenig, J. L. *The Theory of Vibrational Spectroscopy and Its Application to Polymeric Materials*; John Wiley and Sons: New York, Chichester, Brisbane, Toronto, Singapore, 1982.
- (35) Zbinden, R. *Infrared Spectroscopy of High Polymers*; Academic Press: New York, 1964.